MODIFIED DYE-SENSITIZED SOLAR CELL (DSSC) FOR ENHANCEMENT OF PHOTOVOLTAIC PROPERTIES

by

HIDAYANI BINTI JAAFAR

Thesis submitted in fulfillment of the
requirements for the degree of
Doctor of Philosophy

April 2019

ACKNOWLEDGEMENT

Bismillahhirahmanirrohim. Alhamdullilah, with the granted from Allah S. W. T, this thesis can finally be completed.

Firstly, I would like to express my sincere gratitude to my supervisor, Prof. Dr. Hj. Zainal Arifin bin Ahmad for the continuous support of my PhD research and personal life for his patience, motivation, and immense knowledge. His guidance helped me in all the time of research and writing of this thesis. I could not have imagined having a better advisor and mentor for my PhD study. Besides my supervisor, I would like to thank my co-supervisor: Prof. Dr. Mohd Fadzil Ain for his continuous support through his suggestions and guidance in the research and myself developments.

My special thanks to Dean, Assoc. Prof. Ir. Dr. Syed Fuad bin Saiyid Hashim, deputy deans, lecturers and all staffs of School of Materials and Mineral Resources Engineering, Universiti Sains Malaysia (USM) for their kind assistance and support. I am specifically grateful for the technical support from Mr. Shahrul Ami bin Zainal Abidin, Mr. Mohamad Shafiq bin Mustapa Sukri, Mr. Mokhtar bin Mohamad, Mr. Rashid bin Selamat, Mr**.** Kemuridan Bin Md. Desa, Mr. Mohd Azam Bin Rejab, Mr. Muhammad Khairi Bin Khalid, Mr. Mohamad Zaini Bin Saari and Mrs. Hasnah Bt Awang.

I gratefully acknowledge the Ministry of Education, Malaysia and Universiti Malaysia Kelantan (UMK) for their sponsorship through my study under the SLAB/SLAI Scholarship Scheme.

My sincere thanks also goes to my fellow lab mates, Dr. Nik Akmar bin Rejab, Dr. Mohd Fariz bin Abdul Rahman, Mrs. Nor Fatin Khairah binti Bahanurddin and Ms. Erny Raudhoh binti Shafie for the stimulating discussions, for the time we were working together and supporting each other and for all the fun we have.

Last but not least, special thanks to my husband, Wan Mohd Zunaidi bin Wan Deraman and my kid; Wan Muhammad Harith bin Wan Mohd Zunaidi, my parents, Haji Jaafar bin Md. Yusof and Hajah Asmah bt Hedzir and also to my sister, Dr. Haryati binti Jaafar. Thank you for your support and encouragements.

TABLE OF CONTENTS

		Page
ACKNOWLEDGEMENT		ii
TABLE OF CONTENTS		iv
LIST OF TABLES		x
LIST OF FIGURES		xiii
LIST OF ABBREVIATIONS		xviii
LIST OF SYMBOLS		xix
ABSTRAK		xx
ABSTRACT		xxii
CHAPTER ONE: INTRODUCTION		
1.1	Background of Study	1
1.2	Problem Statements	6
1.3	Objectives	8
1.4	Scope of Study	8
CHAPTER TWO: LITERATURE REVIEW		
2.1	Solar Cell	11
2.2	Dye-sensitized solar cells (DSSC)	11
	2.2.1 Operating Principle of DSSC	12
	2.2.2 Photovoltaic Properties	14
2.3	Strategies to Achieve Higher Efficiencies	16
	2.3.1 Increasing Light Harvesting and Charge Collection Efficiencies	16
	2.3.2 Optimizing of Open Circuit Voltage (V_{OC})	17
2.4	Sensitizer (Dye)	18
	2.4.1 Metal Complex Sensitizer	18
	2.4.2 Metal-Free Organic Sensitizer	19
	2.4.3 Natural Dyes Sensitizers	21
	2.4.3.1 Chlorophyll	24

2.4.3.2 Flavonoids 24
2.4.3.3 Carotenoids 25
2.4.3.4 Anthocyanins 26
2.5 *Eleiodoxa conferta* (*E. conferta*) 31
2.5.1 Plant 31
2.5.2 Fruit 31
2.6 *Garcinia atroviridis (G. atroviridis*) 32
2.6.1 Plant 33
2.7 Perspectives for Natural Dye as Sensitizers 34
2.8 TiO_2 as the Photoanode 38
2.8.1 Modification of Photoanode 42
2.8.2 Influence of Thickness Modification 46
2.8.3 Preparation Method of Doped Photoanode 48
2.9 Electrolytes for DSSC 49
2.9.1 Liquid Electrolyte 50
2.9.2 Solid-State Electrolyte 51
2.9.3 Quasi-Solid Electrolyte 51
2.10 Counter Electrode 51
2.10.1 Importance and Role of Counter Electrode 56
2.10.2 Carbon Materials for Counter Electrode 56
2.10.2.1 Amorphous Porous Carbon 57
2.10.2.2 Graphene 58
2.10.2.3 Graphite 59
2.10.2.4 Carbon Black 60
2.10.2.5 Carbon Nanofiber 61
2.11 Controlled Electron Injection and Transport at Materials Interfaces 62
2.11.1 Electron Injection From Dye to Metal Oxide Interface 62
2.11.2 Influence of Dyes on Electron Injection 65
2.12 Fabrication Methods of Semiconductor Coated Electrode 66
2.12.1 Doctor Blading 66

CHAPTER THREE: MATERIALS AND METHODOLOGY

3.1 Experimental Design 68
3.2 Phase I: Evaluation of Natural Dye Sensitizers 69

3.2.1 Preparation of TiO_2 Electrode 71
3.2.2 Preparation of Natural Dye Sensitizers 71
3.2.3 Graphite Coated Counter Electrode 72
3.2.4 Assembly of DSSC 72
3.2.5 Characterization of DSSC 73
3.2.5.1 Infrared Spectroscopy Analysis 73
3.2.5.2 Absorption Spectroscopy Analysis 74
3.2.5.3 Cyclic Voltammetry 74
3.2.5.4 Photovoltaic Properties Measurement 76
3.3 Phase II: Synthesis of Nb-doped TiO_2 Photoanode 77
3.3.1 Preparation of Nb-doped TiO_2 79
3.3.2 Preparation of Photoanode and Assembly of DSSCs 79
3.3.3 Characterization of Nb-doped TiO_2 80
3.3.3.1 Surface Morphology Analysis 81
3.3.3.2 Brunauer–Emmett–Teller (BET) 81
3.3.3.3 Electrochemical Impedance Spectroscopy (EIS) 81
3.4 Phase III: Optimization of Carbon black-TiO_2 Composite Counter Electrode 82
3.4.1 Preparation of Counter Electrode 81
3.4.2 Assembly of DSSC 85

CHAPTER FOUR: RESULTS AND DISCUSSIONS

4.1 Introduction 86
4.2 Phase I: Evaluation of Potential Natural Dye Sensitizers 86
4.2.1 FTIR Spectra 86
4.2.2 UV-vis Absorption 88
4.2.3 Photovoltaic Properties 89
4.2.3.1 Photovoltaic Performance with Different Thicknesses of TiO_2 Layers 90
4.2.3.2 Comparison of Photovoltaic Performances for 3.16 µm Thick TiO_2 Layer 94
4.2.4 Summary from Phase I 97
4.3 Phase II: Determination of Optimum Amount of Nb-doped TiO_2 Photoanode 98

4.3.1 XRD Analysis 98
4.3.2 Optical Properties Analysis 101
4.3.3 FESEM Analysis 103
4.3.4 Photovoltaic Performance of DSSC 107
4.4 Optimization of TiO_2 Doped with Nb 111
4.4.1 XRD Analysis 111
4.4.2 UV-vis Analysis 112
4.4.3 Surface Morphology Analysis 115
4.4.4 Photovoltaic Performance of DSSC 118
4.4.5 Electrochemical Impedance Spectroscopy (EIS) 120
4.4.6 Summary from Phase II 123
4.5 Phase III: Modification of Optimum Composition for Carbon Black-TiO_2 Composite Counter Electrode 123
4.5.1 Modification of Carbon Black-TiO_2 Composite Counter Electrode 123
4.5.1.1 XRD Analysis 124
4.5.1.2 Surface Morphology Analysis 125
4.5.1.3 Photovoltaic Properties 128
4.5.1.4 Electrochemical Impedance Spectroscopy (EIS) 131
4.5.2 Modification of Temperature 133
4.5.2.1 XRD Analysis 134
4.5.2.2 Surface Morphology Analysis 136
4.5.2.3 Photovoltaic Properties 138
4.5.2.4 Electrochemical Impedance Spectroscopy (EIS) 141
4.5.3 Modification of Soaking Time 143
4.5.3.1 XRD Analysis 143
4.5.3.2 Surface Morphology Analysis 144
4.5.3.3 Photovoltaic Properties 147
4.5.3.4 Electrochemical Impedance Spectroscopy (EIS) 149
4.5.4 Summary of Phase III 151
4.6 Integration of Optimum Parameters of DSSC towards Photovoltaic Properties 151

CHAPTER FIVE: CONCLUSION AND RECOMMENDATION

5.1 Conclusion 154

5.2 Recommendation for Future Research 155

REFERENCES 156

LIST OF PUBLICATIONS

LIST OF TABLES

		Page
Table 2.1	Several types of anthocyanins pigments in the visible region	26
Table 2.2	Previous works on photovoltaic performance of natural dyes that contain anthocyanin pigment used in DSSC as sensitizers (TiO_2 as photoanode)	29
Table 2.3	Photoelectrochemical parameters of the DSSC's sensitized with different natural dyes extracted from leaves, seeds, flowers, fruits, vegetables and tree barks	30
Table 2.4	Comparison between synthetic dye and natural dye in DSSC application	35
Table 2.5	The photovoltaic performances of DSSC fabricated with various thickness of TiO_2 thin film	47
Table 2.6	Performance of modified counter electrode in DSSCs	53
Table 2.7	Advantages and disadvantages of carbon materials	57
Table 3.1	Basic ac electrical elements	82
Table 4.1	Photovoltaic performances of DSSCs sensitized with *G. atroviridis* and *E. conferta*	90
Table 4.2	Photovoltaic performances of *E. conferta* coated on different thicknesses of TiO_2 layers	93
Table 4.3	Photovoltaic performances of *G. atroviridis* coated on different thicknesses of TiO_2 layers	93
Table 4.4	Photovoltaic performances of DSSCs of dye extracts at the optimum TiO_2 thickness	95
Table 4.5	Oxidation energy, Energy reduction, HOMO and LUMO measuring with Cyclic Voltammetry	96
Table 4.6	Lattice parameter, average crystallite size and d – spacing of Nb doped TiO_2	100
Table 4.7	Analysis of photon energy for Nb-doped TiO_2	103
Table 4.8	Photovolatic parameters of DSSC fabricated with undoped and Nb doped TiO_2	109

Table 4.9	Lattice parameter, average crystallite size and d – spacing of Nb doped TiO_2	112
Table 4.10	Analysis of photon energy for Nb-doped TiO_2	115
Table 4.11	Analysis of porosity, grain size and surface area	116
Table 4.12	Photovolatic parameters of DSSC fabricated with undoped and Nb doped TiO_2	119
Table 4.13	Properties determined by EIS measurement with different amounts of Nb dopant	123
Table 4.14	Lattice parameter, average crystallite size of 5-20 wt% carbon black-TiO_2 composite	125
Table 4.15	Analysis of grain size, porosity, and surface area of carbon black-TiO_2 composite counter electrode	127
Table 4.16	Photovoltaic parameters counter electrodes based on graphite and different amount of carbon black that annealed at 500 °C and 1 hour soaking time	129
Table 4.17	Properties determined by EIS measurement with graphite and different amounts of carbon black-TiO_2 composite counter electrode	133
Table 4.18	Lattice parameter, average crystallite size of 15 wt% carbon black-TiO_2 composite at 450ºC, 475 °C, 500 °C, 525 °C, and 550 °C annealing temperature with 1 hour soaking time	135
Table 4.19	Analysis of grain size and porosity of 15 wt% carbon black-TiO_2 composite at 450ºC, 475 °C, 500 °C, 525 °C, and 550 °C annealing temperature with 1 hour soaking time	137
Table 4.20	Photovoltaic parameters counter electrodes based on annealing temperature and 1 hour soaking time of 15 wt% carbon black-TiO_2 composite counter electrodes	140
Table 4.21	Properties determined by EIS measurement for different annealing temperature of 15 wt% carbon black-TiO_2 composite counter electrodes and 1 hour soaking time	142
Table 4.22	Lattice parameter, average crystallite size of 15 wt% carbon black-TiO_2 composite with different soaking time	144
Table 4.23	Analysis of grain size and porosity of 15 wt% carbon black-TiO_2 composite at 30 min, 60 min, and 90 min soaking time with 525 °C annealing temperature	145

Table 4.24	Photovoltaic parameters counter electrodes based on based on different soaking time and 525 °C of annealing temperature of 15 wt% carbon black-TiO_2 composite counter electrodes	148
Table 4.25	Properties determined by EIS measurement of counter electrodes based on different soaking time and 525 °C of annealing temperature of 15 wt% carbon black-TiO_2 composite counter electrode	150
Table 4.26	Optimization of parameters for DSSC application	152
Table 4.27	Comparison of photovoltaic properties using natural dye as sensitizer	153

LIST OF FIGURES

		Page
Figure 1.1	Energy band diagram of n-type semiconductor	4
Figure 2.1	Schematic diagram of DSSC	13
Figure 2.2	Photocurrent-voltage of DSSC	15
Figure 2.3	Designed structure of a metal-free organic dye	16
Figure 2.4	Classification of plant pigments	22
Figure 2.5	Chemical structure of commonly occurring flavonoid	25
Figure 2.6	Basic chemical structure of anthocyanin pigment in which 'R' could be replaced with H, OH or OCH_3 depending on the pigment. The numbers can be substituted with hydroxyl group	28
Figure 2.7	*E. conferta* fruit red-skinned, (B) *E. conferta* fruit brown skinned, and (C) *E. conferta* fruit yellow-skinned	32
Figure 2.8	(A) Fruit (B) Flower, and (C) Leave of *G. atroviridis*	34
Figure 2.9	The anatase unit cell; titanium atoms are grey, oxygen atoms are red. Oxygen atoms form a distorted octahedron with a titanium atom at the center, which is clearly illustrated for the central titanium atom	38
Figure 2.10	The rutile unit cell; titanium atoms are grey, oxygen atoms are red	39
Figure 2.11	Crystal structure of brookite	39
Figure 2.12	FESEM image of a nanocrystalline anatase electrode that deposited onto FTO glass	42
Figure 2.13	llustration of how doping a semiconductor to increase its carrier concentration can make it degenerate and highly conductive. E_C is the conduction band minimum, E_F the Fermi level, and E_V the valence band maximum	43
Figure 2.14	Schematic energy band diagram of (a) reference device and (b) DSSCs with Ta-doped TiO_2 photoelectrodes showing the negative shift of conduction band edge	44

Figure 2.15	Schematic representation of spherical anatase TiO_2 nanoparticles based DSSCs, where (A) back electron transfer (recombination) is the major role for loss of conversion efficiency; (B) insertion of another metal oxide as shell or interface modifier also controls the back electron transfer	45
Figure 2.16	(a) Cross-sectional SEM image of TiO_2 film, and (b) J–V curve for DSSC with different TiO_2 film thicknesses	47
Figure 2.17	Schematic illustration of the edge and basal plane of graphite	60
Figure 2.18	SEM images of carbon black with different size (a) 20, (b) 30, (c) 70, and (d) 90 nm (left) and their corresponding EIS results (right)	61
Figure 2.19	Schematic illustration of exciton dissociation of the metal oxide (TiO_2)/dye interface and electron injection into metal oxide	63
Figure 2.20	State diagram representation of the kinetics of DSSC function. Forward processes of light absorption, electron injection, dye regeneration, and charge transport are indicated by blue arrows. The competing loss pathways of excited-state decay to ground and electron recombination with dye cations and oxidized redox couple are shown in black. The vertical scale corresponds to the free energy stored in the charge-separated states	65
Figure 2.21	Schematic diagram (top view) of doctor blade technique	67
Figure 3.1	Flow chart for the preparation of natural sensitizers	70
Figure 3.2	(a) *E. conferta*, and (b) *G. atroviridis* fruits	72
Figure 3.3	(a) The scheme of DSSC assembly process, and (b) working mechanism	73
Figure 3.4	Cyclic Voltammogram and i_{pc} and i_{pa} represents the cathodic and anodic peak current for a reversible reaction	75
Figure 3.5	Flow chart for the preparation of Nb-doped TiO_2 photoanode	78
Figure 3.6	Sintering profile for Nb-doped TiO_2	79
Figure 3.7	Flow chart for the preparation of carbon black-TiO_2 composite counter electrode	84
Figure 4.1	FTIR spectrum of (a) pure TiO_2 (b) *E.conferta* dye sensitized TiO_2, and (c) *G. atroviridis* dye sensitized TiO_2	87
Figure 4.2	Absorption spectrum of natural dyes	88

Figure 4.3	Photocurrent-voltage (J-V) characteristics of dye extracted from (a) *E. conferta*, and (b) *G. atroviridis*	90
Figure 4.4	FESEM images of TiO_2 in three different thicknesses on FTO glass (a) 1.83 µm (1 layer of adhesive tape), (b) 3.16 µm (2 layers of adhesive tape), and (c) 7.60 µm (3 layers of adhesive tape)	92
Figure 4.5	Comparison of photocurrent voltage (J–V) characterizations of *E. conferta* coated on different thicknesses of TiO_2 layers (a) 1.83 µm, (b) 3.16 µm, and (c) 7.60 µm	92
Figure 4.6	Comparison of photocurrent voltage (J–V) characterizations of *G. atroviridis* coated on different thicknesses of TiO_2 layers (a) 1.83 µm, (b) 3.16 µm, and (c) 7.60 µm	93
Figure 4.7	Chemical structure for a) *G. atroviridis* (Mackeen et al., 2012), (b) *E. conferta*	96
Figure 4.8	Cyclic-voltammetry plot of (a) *E. conferta*, and (b) *G. atroviridis*	96
Figure 4.9	Schematic diagram showing the calculated positions of HOMO and LUMO levels of anthocyanins extracted from *G. atroviridis* and *E. conferta*	97
Figure 4.10	(a) XRD patterns of 0-5 wt% Nb doped TiO_2, and (b) Shifts in peak position and changes in peak broadening are depicted through enlarge view of (101) peaks for undoped TiO_2 and Nb doped TiO_2	100
Figure 4.11	(a) The UV-vis absorbance spectra of DSSC based on the Nb doped TiO_2 with different Nb contents	102
Figure 4.12	Plots of $(\alpha hv)^{1/2}$ versus photon energy Nb-doped TiO_2 at (a) 0 wt% Nb (b) 1.0 wt% Nb (c) 1.5 wt% Nb (d) 2.0 wt% Nb (e) 2.5 wt% Nb (f) 3.0 wt% Nb (g) 3.5 wt% Nb (h) 4.0 wt% Nb (i) 4.5 wt% Nb, and (j) 5.0 wt% Nb	103
Figure 4.13	FESEM images for (a) 0 wt% Nb, (b) 1.0 wt% Nb, (c) 1.5 wt% Nb, (d) 2.5 wt% Nb, (e) 3.5 wt% Nb, (f) 4.5 wt% Nb, and (g) 5.0 wt% Nb	105
Figure 4.14	Grain size and porosity analysis 0 wt% Nb, 1 wt% Nb, 1.5 wt% Nb, 2.5 wt% Nb, 3.5 wt% Nb, 4.5 wt% Nb, and 5 wt% Nb	107
Figure 4.15	Illustration of Nb and dye injection into photoanode	107
Figure 4.16	The photocurrent density–photovoltage (J–V) of the fabricated DSSC using undoped (0 wt% Nb), and Nb-doped TiO_2 (1.0-5.0 wt% Nb)	108

Figure 4.17	(a) XRD patterns of 0-1.75 wt% Nb doped TiO_2, and (b) Shifts in peak position and changes in peak broadening are depicted through enlarge view of (101) peaks for undoped TiO_2 and Nb doped TiO_2	112
Figure 4.18	Absorbance spectra of DSSC based on the Nb-doped TiO_2 with different Nb contents	113
Figure 4.19	Plots of $(\alpha hv)^{1/2}$ versus photon energy for Nb-doped TiO_2 at (a) 0 wt% Nb (b) 0.25 wt% Nb (c) 0.5 wt% Nb (d) 1.0 wt% Nb (e) 1.25 wt% Nb (f) 1.5 wt% Nb, and (g) 1.75 wt% Nb	114
Figure 4.20	FESEM images of a) 0 wt% Nb-doped TiO_2, b) 0.25 Nb-doped TiO_2, c) 0.5 wt% Nb-doped TiO_2, d) 1.0 wt% Nb-doped TiO_2, e) 1.25 wt% Nb-doped TiO_2, f) 1.5 wt% Nb-doped TiO_2, and g) 1.75 wt% Nb-doped TiO_2	117
Figure 4.21	Correlation between grain size and surface area at 0 wt% Nb, 1.0 wt% Nb, and 1.5 wt% Nb	118
Figure 4.22	The photocurrent density – photovoltage (J – V) of the fabricated DSSC using undoped and Nb doped TiO_2	119
Figure 4.23	Nyquist plots of DSSCs measured under illumination conditions for undoped and Nb-doped TiO_2	122
Figure 4.24	XRD patterns of 5-20 wt% carbon black-TiO_2 composite	125
Figure 4.25	Surface morphology images for carbon black-TiO_2 composite counter electrode at (a) 0 wt% carbon black-TiO_2 (b) 5 wt% carbon black-TiO_2 (c) 10 wt% carbon black-TiO_2 (d) 15 wt% carbon black-TiO_2, and (e) 20 wt% carbon black-TiO_2 that annealed at 500 °C and 1 hour soaking time	127
Figure 4.26	Correlation between grain size and surface area analysis for carbon black-TiO_2 composite	128
Figure 4.27	J-V curves of counter electrodes based on graphite and different amount of carbon black counter electrode that annealed at 500 °C and 1 hour soaking time	129
Figure 4.28	Nyquist plots of DSSCs measured under illumination conditions for different amount of carbon black-TiO_2 composite and graphite	132
Figure 4.29	XRD patterns of 15 wt% carbon black-TiO_2 composite at 450ºC, 475 °C, 500 °C, 525 °C, and 550 °C annealing temperature with 1 hour soaking time	135
Figure 4.30	Surface morphology images for 15 wt% carbon black-TiO_2 composite at (a) 475 °C (b) 500 °C (c) 525 °C (d) 550 °C annealing temperature with 1 hour soaking time	137

Figure 4.31	Grain size and porosity analysis for 15 wt% carbon black-TiO_2 composite at 475 °C, 500 °C, 525 °C, and 550 °C annealing temperature with 1 hour soaking time	138
Figure 4.32	J-V curves of counter electrodes based on different annealing temperature and 1 hour soaking time of 15 wt% carbon black-TiO_2 composite counter electrodes	139
Figure 4.33	Condition of carbon black-TiO_2 composite counter electrode after annealed at different annealing temperature	141
Figure 4.34	Nyquist plots of DSSCs measured under illumination conditions for different annealing temperature of 15 wt% carbon black-TiO_2 composite counter electrodes	142
Figure 4.35	XRD patterns of 15 wt% carbon black-TiO_2 composite with different soaking time	144
Figure 4.36	Surface morphology images for 15 wt% carbon black-TiO_2 at (a) 30 min (b) 60 min (c) 90 min soaking time with 525 °C annealing temperature	146
Figure 4.37	Grain size and porosity analysis for 15 wt% carbon black-TiO_2 composite at 30 min, 60 min, and 90 min soaking time with 525 °C annealing temperature	146
Figure 4.38	J-V curves of counter electrodes based on different soaking time and 525 °C of annealing temperature of 15 wt% carbon black-TiO_2 composite counter electrodes	148
Figure 4.39	The condition of carbon black-TiO_2 composite counter electrode assembled for DSSC testing at different soaking time	149
Figure 4.40	Nyquist plots of DSSCs measured under illumination conditions for different soaking time and 525 °C of annealing temperature of 15 wt% carbon black-TiO_2 composite counter electrode	150

LIST OF ABBREAVIATIONS

AM	Air Mass
BET	Brunauer–Emmett–Teller
BM	Burstein-Moss
CB	Conduction band
DSSC	Dye-sensitized solar cells
EIS	Electrochemical Impedance Spectroscopy
FESEM	Field Emission Scanning Electron Microscopy
FTIR	Fourier Transform Infrared
HOMO	Highest occupied molecular orbital
LUMO	Lowest unoccupied molecular orbital
PV	Photovoltaic
UV-vis	Ultraviolet–visible
UV	Ultraviolet
WEO	World Energy Outlook
XRD	X-ray Diffraction

LIST OF SYMBOLS

V_{OC}	Open circuit voltage
η	Energy conversion efficiency
J_{SC}	Short-circuit current density
FF	Fill factor
I_{SC}	Short circuit current
°	Degree
°C	Degree Celsius
%	Percentage
E_g	Band gap
m^2/g	Surface area
R_{CE}	Charge-transfer resistance at counter electrode/electrolyte interface
R_{CT}	Charge-transfer resistance at photoanode/dye/electrolyte interface
Ω	Ohm
R_S	Series resistance

PENGUBAHSUAIAN SEL SURIA TERSINTESIS DAI (DSSC) UNTUK PENINGKATAN CIRI-CIRI FOTOVOLTIK

ABSTRAK

Sel suria tersintesis dai (DSSC) menjanjikan peranti fotovoltik berkos rendah yang mempunyai peluang untuk menjadi pesaing kepada sel suria yang berasaskan teknologi persimpangan p-n. DSSC difabrikasikan dari bahan yang murah melalui proses yang mudah dan mungkin menjadi penyumbang penting kepada pengkomersialan teknologi fotovoltik di masa hadapan. Oleh itu, dengan menggunakan dai semulajadi sebagai pemeka adalah salah satu cara untuk mengurangkan kos fabrikasi DSSC. Walau bagaimanapun, kecekapan (η) menggunakan dai semulajadi masih rendah (< 2%) berbanding teknologi yang sedia ada. Oleh itu, matlamat kajian ini dijalankan adalah untuk mengoptimumkan keupayaan DSSC dengan mengenalpasti dai semulajadi yang paling sesuai digunakan sebagai pemeka dan digabungkan dengan penambahbaikan melalui pengubahsuaian fotoanod dan elektrod bertentangan untuk meningkatkan sifat fotovoltik menggunakan dai semulajadi. Terdapat empat fasa dalam kajian ini. Fasa pertama, *E. conferta* dan *G. atroviridis* dipilih sebagai dai semulajadi yang akan digunakan sebagai pemeka. Usaha untuk meningkatkan prestasi peranti dijalankan dan pada masa yang sama menggunakan pemeka yang dihasilkan dengan kos yang rendah. *E. conferta* dipilih berdasarkan ciri-ciri fotovoltik yang lebih bagus dan menghasilkan η (1.18%) lebih tinggi berbanding dengan G. *atroviridis* (0.85%). Dalam fasa kedua, pengubahsuaian fotoanod bagi peningkatan ciri-ciri fotovoltik menggunakan *E. conferta* dengan jumlah Nb-dop TiO_2 (0-5 wt% Nb) yang berbeza disintesis menggunakan kaedah tindak balas keadaan pepejal. 1.0 wt% Nb-dop TiO_2 meningkatkan η kepada 1.4%. Dalam fasa ketiga, tiga pemboleh ubah iaitu perbezaan jumlah karbon hitam, perbezaan suhu sinter dan perbezaan masa sinter

dijalankan terhadap karbon hitam-TiO_2 komposit elektrod bertentangan. DSSC berasakan 15 wt% karbon hitam-TiO_2 komposit elektrod bertentangan menghasilkan η yang tertinggi (2.5%) dengan menggunakan *E. conferta* sebagai pemeka. Apabila pengubahsuaian suhu sinter dijalankan pada suhu 525 °C selama 1 jam, η bertambah kepada 2.77%. Oleh itu, dengan menggunakan *E. conferta* sebagai pemeka semulajadi, η meningkat menghampiri 3% bersama pengubahsuaian fotoanod menggunakan 1.0 wt% Nb-dop TiO_2 dan 15 wt% karbon hitam-TiO_2 komposit elektrod bertentangan yang disinter pada suhu 525 °C dan 1 jam masa disinter.

MODIFIED DYE-SENSITIZED SOLAR CELL (DSSC) FOR ENHANCEMENT OF PHOTOVOLTAIC PROPERTIES

ABSTRACT

Dye-sensitized solar cells (DSSC) are promising low-cost photovoltaic devices that have a good chance to become a competitor to p-n junction solar cells based technology. DSSCs are fabricated from abundant and cheap materials via inexpensive processes and are likely to be a significant contributor to the future commercial photovoltaic technology. Therefore, by using natural dyes as sensitizers is one of the alternative ways to reduce the fabrication cost of DSSC. However, the efficiency (η) of these natural dyes is still low (<2 %) compared to the existing solar cell technology. Therefore, the aim of this work is to optimize DSSC capability by identifying the most suitable natural dyes to be used as sensitizers and coupled with further improvement through the modification of both photoanode and counter electrode in order to enhance the photovoltaic properties using natural dye. There are four phases in this study. For first phase, *E. conferta* and *G. atroviridis* were selected as natural dyes to be used as sensitizers. Efforts are tried to enhance the device performance but at the same time used of low cost sensitizers. *E. conferta* has been selected due to better photovoltaic properties and produced better η (1.18%) compared to *G. atroviridis* (0.85%). In second phase, modification of photoanode for enhancement of photovoltaic properties using *E. conferta* with different amount Nb-doped TiO_2 (0–5 wt% of Nb) were synthesized via solid state technique. By doping with 1.0 wt% Nb-doped TiO_2, the η increased to 1.40%. In third phase, further modification in counter electrode using carbon black-TiO_2 composite was investigated. In this phase, three parameters were varies which are different amount of carbon black, different sintering temperature and different sintering time for carbon black-TiO_2 composite counter electrode. DSSC-based on 15 wt% of carbon

black-TiO_2 composite counter electrode reached the highest η (2.5%) by using *E. conferta* as sensitizer. Upon modification of sintering parameter at 525 °C for an hour, η increased to 2.77%. Therefore, by using *E. conferta* as natural sensitizer, η has increased to almost 3% when integrated with modified photoanode (1.0 wt% Nb-doped TiO_2) and counter electrode (15 wt% carbon black-TiO_2 composite that sintered at 525 °C for an hour).

CHAPTER ONE

INTRODUCTION

1.1 Background of Study

Electricity is the set of physical phenomena associated with the presence and flow of electric charge (Solanki, 2013). In facts, electricity is a secondary energy which meant users must use the other primary sources of energy to generate the electricity. Primary sources of energy can be harnessed and refined from a wide range of sources and be used for a diverse uses. There are two types of energy resources in this world which are non-renewable and renewable resources.

Energy of non-renewable resource is energy that produced from nuclear and fossil fuels such as coals, natural gaseous and petroleum. These energy resources are called as non-renewable resources because the resources cannot be replaced or will be replaced through a very slow natural process. On the other hand, renewable resources are the opposite to non-renewable resources. Energy from renewable resources is actually energy which come from natural resources and does naturally replenished. The examples of renewable energy are wind energy, biomass energy, solar energy and hydro energy. Renewable energy resources are alternative resource to fossil fuels and nuclear power. The most important thing in utilising these renewable resources is application of ecofriendly technologies which give less negative impact to environment and also society.

Motivated by continuously growing global energy demands and the depletion of readily accessible fossil fuels; the search for alternative energy sources, particularly renewable solar energy, has become more aggressive. Despite the clear advantages associated with the adoption of solar cells, they need to be cost-effective

and priced competitively in comparison to conventional energy resources, as any technological or performance improvements must be balanced against the associated cost (Chaar et al., 2011). Since significant breakthroughs in 1991 (O'regan et al., 1991), dye-sensitized solar cells (DSSCs) have entered public view and garnered more attention over the following 30 years.

The efficiency and cost of DSSC depends on each part of the device. Therefore, in past years many researchers focused on the modification of each component in DSSC. Many areas such as construction of nanostructured semiconductor photoanodes with effective design for high dye loading and fast electron transfer, the exploitation of various sensitizers that have strong light harvesting ability, the utilization of redox electrolytes with useful compositions for efficient hole transfer and the optimization of the low cost development of counter electrode were explored in order to find the better result for DSSC.

DSSCs that use dye molecules to absorb photons and convert them to electric charges, drawn a lots of attention due to their easy fabrication, low cost and the comparatively better energy conversion efficiency (Gratzel et al., 2003; Ito et al., 2007). A conventional of DSSC made of a dye activated mesoporous semiconductor oxide film on conducting glass, an iodine electrolyte solution and a platinized counter electrode (Amoli et al., 2015). For the conventional silicon solar cells, the semiconductor takes charge of both the photon absorption and charge transport.

Meanwhile, in DSSCs, light is absorbed by the sensitizer (dye) and transfer the electron injection from the sensitizer to the conduction band of the semiconductor. There are several ways to enhance the performance of DSSCs which are (a) increase of light harvesting that can be achieved with good surface area and

absorption of broader range of solar light (Huang et al., 2012), (b) increase of the electron injection speed by improving the electron injection over potential (Koops et al., 2009), (c) moving the redox couple Fermi level to enhance the dye regeneration rate (Feldt et al., 2011; Wang et al., 2012), (d) enhancing the lifetime of electrons by retarding the probability of charge recombination (Santiago et al., 2005) and (e) improving the charge transfer rate in TiO_2 (Liu et al., 2010; Lu et al., 2010).

Nanostructured semiconductor films are the base of DSSC photoanodes. The photoanode provides function to support the sensitizer loading and transfer the photoexcited electrons from sensitizers to external circuit. Thus, large surface area is required to ensure high dye loading. To ensure the transferring of photoexcited electron, anatase titanium dioxide (TiO_2) has been widely used as photoanode. Due to its outstanding optical and electrical properties, TiO_2 has been extensively investigated as one of the most promising wide band gap semiconducting materials in photocatalysis (Asahi et al., 2001; Tian et al., 2008) and photovoltaic applications (Han et al., 2011). For instance, TiO_2 nanoparticles with large surface areas are often employed in dye-sensitized solar cells (DSSC) (Sun et al., 2012; Mali et al., 2013). However, polycrystalline structures result in disordered networks that impede charge transport and lead to the recombination of photo-generated electrons and holes (Melhem et al., 2013). As a result, single-crystal TiO_2 is preferred, for it can provide direct electrical pathways for photo-generated charges and avoid electron scattering or trapping (Zhou et al., 2011). When electron transport is oriented, the DSSCs can enhance performance in photoelectric conversion.

Modification of photoanode in previous studies with TiO_2 based photoanode have shown that doping TiO_2 with various metals could enhance some of the photovoltaic properties of the cell. There are advantages in DSSCs by doping the

TiO_2 semiconductor which is reduction in band gap that increased the efficiency, and reduction in electron/electrolyte recombination. Doping can be achieved by either replacing the Ti^{4+} cation or the O^{2-} anion. Cationic dopants are typically metals, whereas anionic dopants are non-metals. As shown in Figure1.1, the dopant atoms produce the majority carriers and filled the donor level are excited to move to the conduction band. The energy level of the donor (E_D) is lower than the conduction band (E_C). Hence, electrons can move into the conduction band with minimal energy. Also, when the sun directly applied to the DSSC, most donor atoms and very few Ti atoms get ionized and the donor atom will move into the conduction band. The conduction band has most electrons from the donor impurities. Therefore, doping is an effective strategy to tune the band gap of TiO_2 by introducing new energy levels in between and by alteration of conduction band minima (CBM) and valence band maxima (VBM). Decrease in the band gap energy involves an increase in the open-circuit voltage (V_{OC}) of the DSSC since the band gap energy is one of the factors affecting the V_{OC} in this type of photovoltaic devices.

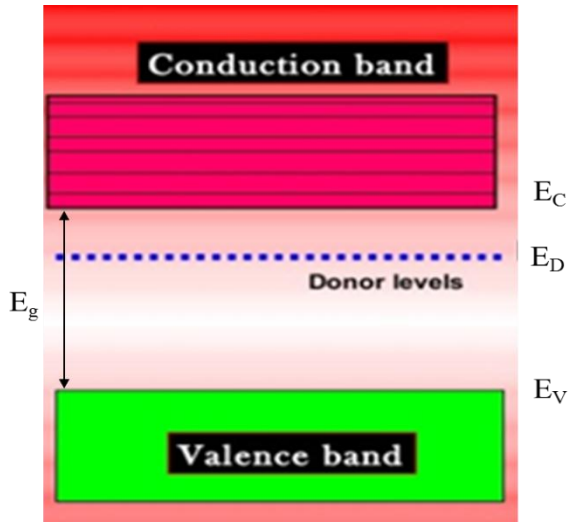

Figure 1.1: Energy band diagram of n-type semiconductor

The sensitizer is the central component in DSSC due to it harvest sunlight and produces photo-excited electrons at the semiconductor interface. Therefore, widely investigation on the easily available dyes extracted from natural sources as a photosensitizers were conducted due to their large absorption coefficients, high light harvesting efficiency, low cost, easy preparation, environment friendliness and nearly match with the CB of TiO_2 (Chang et al., 2010; Li et al., 2013; Maabong et al., 2015). *E. conferta* and *G. atroviridis* have been selected in this study due to the anthocyanin pigment that consists in these fruits. Two groups that present in the anthocyanins molecule, carbonyl and hydroxyl, can be bounded to the surface of the porous TiO_2 film. This makes electron transfer from the anthocyanin molecule to the CB of TiO_2 feasible (Garcia et al., 2003). Compared to the N719 dye (-3.01 eV), the LUMO level of anthocyanin also nearly matched with the CB of TiO_2 (-3 to -3.86 eV) (Suyitno et al., 2015). The conduction band (CB) has to match the lowest excited state of the dye molecule to enable effective electron transfer from the molecule's excited state to the semiconductor's conduction band. This is to allow for efficient charge injection into the TiO_2 to achieve an efficient regeneration of the oxidized dye and recombination prevention (the electrons in the TiO_2 recombine either with the oxidized dye or the redox electrolyte) (Yella et al., 2011).

Counter electrode (CE) is one of the major components in DSSC. CE acts as a catalyst by reducing the redox species, which are the mediators for regenerating the sensitizer after the electron injection. The reactions at the CE mainly depend on the redox species used to transfer electrons between the photoanode and the CE. Usually, an I^-/I_3^- couple is used as the redox mediator in DSSC. A CE material in a DSSC should possess a high catalytic activity and stability towards the electrolyte used in the cell. Usually, platinum (Pt)-coated fluorine-doped tin oxide (FTO) is used

as a counter electrode owing to its superior catalytic activity. However, there are researches reporting that Pt corrodes in an electrolyte containing iodide to generate PtI_4 (Ohmukai et al., 2014). Besides, large solar module systems will benefit from materials that are abundantly available with high chemical stability. Therefore, it is necessary to develop alternative materials which must be inert and show good catalytic effect in the electrolyte. A great deal of effort has been taken to replace the Pt metal with other materials such as titanium nitrides (TiN) (Choi et al., 2011), and carbon derivatives (Wang et al., 2012). Among these candidates, carbon materials obtain increasing attention due to their abundance, low cost, electrically conducting and show catalytic activity for the reduction of triiodide (Ramasamy et al., 2007). The lower intrinsic catalytic activity of carbon compared to Pt is compensated by the considerably larger active surface area of the electrode structure that characterizes porous carbon materials, providing a large number of reduction sites and hence low charge transfer resistance. Carbon and TiO_2 combine to produce a composite material possessing the combined property of good photocatalytic activity leading to an enhanced effect of photovoltaic (Chia et al., 2015). Carbon is selected as CE due to its electrocatalytic activity and excellent stability towards the I^-/I_3^- electrolyte. A counter electrode must be catalytically active for a rapid reaction and reduce the overpotential. The overpotential is required to drive the reaction at a certain current density, which gives rise to a charge transfer resistance (R_{CT}).

1.2 Problem Statements

Recently, the good efficiency of 12.3 % has been achieved in DSSCs using TiO_2 as a photoanode material, Ru as a sensitizer and Pt as counter electrode. However, the production processes for these solar cells are complicated and expensive which created a demand to search for an alternative technology.

Therefore, by using natural dyes as sensitizer is one of the alternative ways to reduce the fabrication cost of DSSC. However, the value of η of DSSCs using natural dyes is rather too low (<2%) compared to other generations of solar cell (Maurya et al., 2016). To address these issues, wide investigations on the easily available dyes extracted from natural sources as sensitizers were conducted due to their high light harvesting efficiency, low cost, easy preparation, nearly match with the CB of TiO_2 and environment friendliness.

Focusing on semiconductor photoanode, TiO_2 is one of the most important and attractive semiconducting materials that used in DSSCs. Unfortunately, the main downside of TiO_2 is large band gap of TiO_2 (> 3 eV). This material can only absorb the ultraviolet (UV) part of solar emission. For this purpose, by altering the band gap is an effective way to enhance its electrical and optical properties. Since the lower edge of the conduction band (CB) is made up of Ti^{4+} 3d bands, replacing Ti^{4+} by a different cation is thus expected to heavily affect the CB structure. Benefit of metal doping with a valency higher than Ti^{4+} such as Nb^{5+} are to increase free charges, change of electrical conductivity, charge transfer kinetics, and dye absorption characteristics of TiO_2.

In counter electrode, Pt has been widely used as counter electrode in DSSCs due to its superior electrocatalytic activity toward the reduction of I_3^- and excellent electrical conductivity (Calogero et al., 2011; Wu et al., 2012). However, Pt may limits the potential large scale application of DSSCs due to it is an expensive metal and their corrosion in liquid electrolyte is a concern. Furthermore, there are researchers reporting that Pt corrodes in an electrolyte containing iodide to generate PtI_4 (Murakami et al., 2006).

1.3 Objectives

The objectives in this study are:

i. To characterize dye sensitizers from *G. atroviridis* and *E. conferta.*

ii. To determine the photovoltaic properties of Nb-doped TiO_2 photoanode using natural dye.

iii. To investigate variation of carbon black-TiO_2 composite counter electrode for enhancement of DSSC photovoltaic properties

1.4 Scope of Study

Basically, this study was divided into 3 phases which are:

i. Evaluation of photovoltaic properties of DSSC dye sensitizers derived from *G. atroviridis* and *E. conferta.*

ii. Determination of photovoltaic properties using Nb-doped TiO_2 photoanode with natural dye as sensitizer.

iii. Optimization of carbon black-TiO_2 composite counter electrode for enhancement of DSSC photovoltaic properties.

Phase I – Evaluation of Potential Natural Sensitizers

In Phase I, *E. conferta* and *G. atroviridis* were extracted and used as a sensitizer for DSSC without further purification. The flesh of *E. conferta* and *G. atroviridis* were separated from the seed and completely dried at room temperature. The flesh was crushed to powder form using a mortar. The powder was put into a beaker and added with ethanol and stirred. The mixture was left for 24 hours in dark at room temperature. The solid residues of the mixture were filtered out to obtain a pure and clear natural dye solution. The extracted dyes were characterized by ultraviolet–visible (UV–vis) and Fourier Transform Infrared (FTIR) spectroscopy.

The photovoltaic performance (open circuit voltage (V_{OC}), short-circuit current density (J_{SC}), fill factor (FF), and energy conversion efficiency (%) of the fabricated DSSCs were investigated by using these extracts as sensitizers.

Phase II – Synthesis of Nb-doped TiO_2 Photoanode

Modification of photoanode was conducted in Phase II, which added dopant into TiO_2. In Phase II, Nb-doped TiO_2 as a photoanode prepared by using solid-state method with dye extracted that obtained from the Phase I. The amount of Nb varies and mixed with TiO_2 respectively. Nb-doped TiO_2 were sintered and characterized in order to get single crystal structure. TiO_2 paste was prepared by mixed with acetic acid, deionized water, ethanol and Triton–X and ground until get the homogenous paste. TiO_2 pastes were deposited onto FTO glass using doctor blade technique and sintered. Same method was applied for Nb-doped TiO_2 paste. The sintered photoanode electrodes were immersed into natural dye that obtained from Phase I. Next, the DSSC was assembled with graphite counter electrode and a drop of electrolyte and sealed with slurry tape. The mechanism that caused by Nb doping with natural dye as sensitizers that extracted from Phase I were investigated based on phase analysis, surface morphological, electronic and optical behaviors.

Part III – Optimization of Carbon black-TiO_2 Counter Electrode

In Phase III, the optimum results that achieve from Phase I and Phase II will be remained while modification of counter electrode was conducted. Carbon black was used in this phase with varies composition and mixed with TiO_2. The carbon black paste prepared by mixed the mixture (Carbon black + TiO_2) with 10mM H_2PtCl_6 solution in ethanol respectively until homogenous paste was formed. The paste was spread the paste onto FTO glass using doctor blade technique and sintered.

Same method was obtained for different sintering temperature and sintering time. Characterizations were conducted to find the best and the highest efficiency for the DSSC.

CHAPTER TWO

LITERATURE REVIEW

2.1 Solar Cell

Solar cell also known as solar photovoltaic (PV) that converts solar energy into electricity by the PV effect. Solar technologies mainly used the sunlight's radiation to move the negative and positive charge carriers inside absorbing materials. With the presences of electrical field, these charges can produce electrical current and can be used in external circuit (Tiwari et al., 2010). Solar energy is abundant, non-polluting, and able to provide a significant fraction of global energy demand. Current trends suggest that solar energy will play an essential role in future energy production. Perhaps the most promising renewable energy is solar energy, as it can potentially meet the world's energy consumption.

2.2 Dye-sensitized solar cells (DSSC)

O'Regan et al. (1991) began the DSSC with 7% efficiency cell containing a ruthenium as a dye, TiO_2 as photoanode and an iodide/triiodide redox couple as electrolytes. The efficiency of this cell was high due to slow rate of back electron transfer from TiO_2 into the oxidized dye or triiodide (I_3^-). DSSC is an electrochemical solar cell which serves as a medium in converting absorption of light or sun energy directly into electrical power. DSSCs are alternative potentially low-cost PV devices alternative to p-n electrode. They consists of a sensitizing dye, nanoporous metal oxide, an electrolyte and a counter electrode (Baglio et al., 2011).

On the other hand, DSSC have some operation steps to produce the electricity from solar energy. The steps are excitation, injection, diffusion in TiO_2,

iodine reduction and dye regeneration (Wang et al., 2009). There are some best possible chemical functional groups that are able to bind with the TiO_2. The functioning groups are phosphoric acids and carboxylic acids including their derivatives such as acid chlorides, amides, esters or carboxylate acids.

Numerous metal complexes and organic dyes have been synthesized and utilized as sensitizers. By far, the highest efficiency of DSSC sensitized by Ru-containing compounds absorbed on nano crystalline TiO_2 reached 11–12% (Bagher, 2014). However, noble metals limited in amount, and costly in production. On the other hand, organic dyes are not only cheaper but have also been reported to reach efficiency as high as 9.8% (Zhang et al., 2009). However, organic dyes have often presented problems as well, such as complicated synthetic routes and low yields. Nonetheless, the natural dyes found in flowers, leaves and fruits can be extracted by simple procedures. Nowadays, research in DSSC increasing due to DSSC is the best way to maintain and sustain the environment. Important to realize that DSSCs technology will be an important renewable energy source in future if some technology breakthroughs are made (Chu, 2011).

2.2.1 Operating Principle of DSSC

DSSC is a semiconductor device that operates under the conversion of solar radiation to electrical energy as shown in Figure 2.1 (Shalini et al., 2015). It consists multiple components such as a) transpiring conducting oxide (TCO) which usually use fluorine doped tin oxide (FTO) or indium doped tin oxide (ITO), b) mesoporous metal oxide layer that act as photoanode that developed from TiO_2, c) sensitizers (dye molecules), d) electrolyte, mostly used iodide/triiodide (I^-/I_3^-) electrolyte, and e) the last is counter electrode. Inside the DSSC, the sensitizers that absorbed on the surface of mesoporous TiO_2 layer absorbed the incident photons and gets excited

from the ground state (S) to the excited state (S^*). One type of photoexcitation, causes transfer of an electron from the highest occupied molecular orbital (HOMO) of the sensitizers to the lowest unoccupied molecular orbital (LUMO). These excited sensitizers inject an electron into the conduction band of the mesoporous photoanode network and the sensitizers that loose an electron gets oxidized (Yacobi, 2003). In order to reach the counter electrode, the injected electrons travel through TiO_2 layer to the external load. These electrons are transferred to the electrolyte where the oxidized dye receives electron from iodide (I^-) ion to replace the lost electron and simultaneously, the iodide molecules are oxidized to triiodide ions (I_3^-) (Wu et al., 2010). Finally, regeneration of I^- ion takes place at counter electrode (cathode) and migration of electron through the external load completes the circuit (Gong et al., 2012). Overall process of DSSC, the device generates electric power from light without suffering from any permanent chemical transformation. The electron transfer in DSSC needs to be ongoing in order to continually yield the electric power.

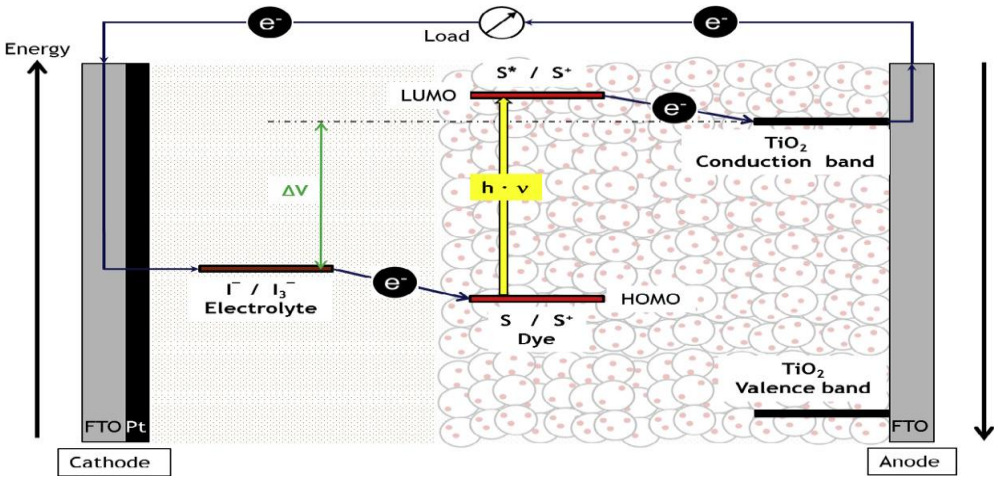

Figure 2.1: Schematic diagram of DSSC (Shalini et al., 2015)

2.2.2 Photovoltaic properties

A DSSC can be characterized with an IV-diagram where the corresponding current (I) at rising voltage (V) is plotted as shown in Figure 2.2. At a bias of 0 V the short circuit current (I_{SC}) is measured and when the current reaches 0 A the open circuit voltage (V_{OC}) is defined. The maximum power output (P_{max}) that generate by DSSC is obtained when the product of the current and voltage is maximum. Based on Equation 2.1, the maximum power is calculated.

$$P_{max} = I_{max} \times V_{max} \quad (2.1)$$

The I_{SC} is the current flows through the external circuit when the electrodes of the DSSC are short circuited. The I_{SC} depends on the photon flux incident on the solar cell which is determined by the spectrum of the incident light. For standard measurement, the spectrum is standardized to the air mass (AM) where 1.5 is refers to path length through the atmosphere. AM1.5 spectrum is the standard air mass value that has been used all over the world. The I_{SC} also depends on the area of working electrode. In order to remove the dependence of the solar cell area onto $I_{SC,}$ the short-circuit current density (J_{SC}) is used to describe the maximum current delivered by the solar cell. The J_{SC} obtained using Equation 2.2. The maximum current that delivered by solar cell strongly depends on the optical properties of the solar cell such as absorption in the absorber layer and reflection. High value of J_{SC} is associated with the following characteristics:

a) Intense light absorption capabilities of dyes over a wide range of sunlight
b) High electron-injection efficiencies from photoexcited dyes to the conduction band of TiO_2
c) Efficient reduction of the oxidized dye by I^-

$$J_{SC} = \frac{I_{SC}}{Area} \tag{2.2}$$

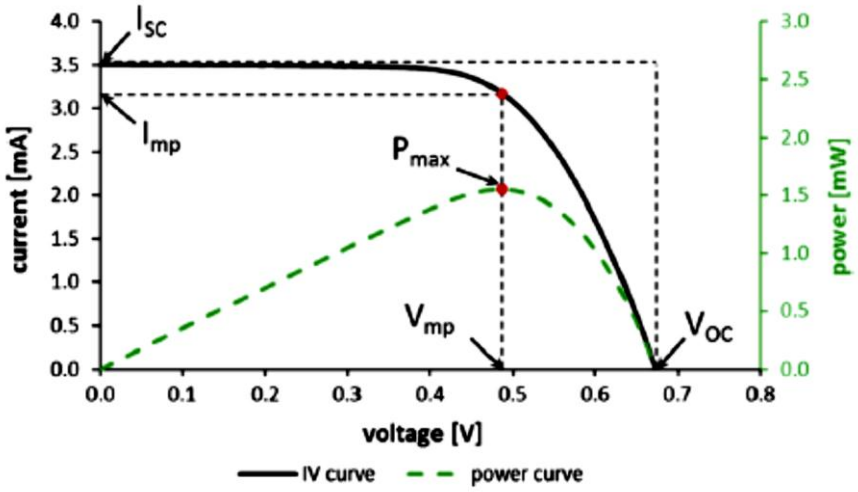

Figure 2.2: Photocurrent-voltage of DSSC (Hubert et al., 2014)

The V_{OC} is the voltage at which no current flows through external circuit. It is the maximum voltage that solar cell can delivered. The V_{OC} corresponds to the amount of forward bias voltage on the solar cell due to the bias of solar cell junction with the light-generated current. Basically, the V_{OC} value is determined by the energy band gap between the Fermi level of the TiO_2 electrode, which is located near the conduction band edge (E_{CB}) and the redox potential of the I^-/I_3^- in the electrolyte as shown in Figure 2.1.

Meanwhile, *FF* is the ratio between the maximum power and the product of I_{SC} and V_{OC} as shown in Equation 2.3. The *FF* is partially determined by the shunt and series resistance of the solar cell. The shunt resistance is not only related with interfacial charge recombination but with charge recombination at FTO/electrolyte interface. The series resistance can be reduced for example by reducing the electrolyte thickness and by increase the counter electrode surface area (Han et al.,

2005). The *FF* also can be related to potential dependent electron transfer/transport rate under light irradiation (Tachibana et al., 2002).

$$FF = \frac{P_{\max}}{V_{OC} \times I_{SC}} \tag{2.3}$$

The efficiency of the solar cells used in PV system determines the annual energy output of the system. The energy conversion efficiency determined how efficient a solar cell can convert the power of the incident light into electricity. The solar energy to electricity conversion efficiency (η) is calculated based on Equation 2.4 where P_{in} is the power of incident light (100 mW/cm^2 as the standard cell irradiation condition).

$$\eta = \frac{(V_{OC})(J_{SC})(FF)}{P_{in}} \times 100 \tag{2.4}$$

2.3 Strategies to Achieve Higher Efficiencies

The development of a DSSC is based on the enhancement of the light to electric energy conversion efficiency and the long time stability (Jung et al., 2013). All the approaches to achieve higher DSSC efficiencies look for the improvement in J_{SC}, V_{OC}, or FF.

2.3.1 Increasing Light Harvesting and Charge Collection Efficiencies

Several approaches have been reported to increase the efficiency of DSSC where one of them is the redesign of the sensitizer molecular structure (Mishra et al., 2009; Lee et al., 2015). This redesign would be focused on enhancing the extinction coefficient of the dye at the red part of the spectrum, where the density of photons from the sun is higher (Hagfeldt et al., 2010). Even with these improvements in the

structure of the dye, the aggregation effect on the semiconductor film could reduce the photocurrent that decreases the electron injection efficiency. Therefore, the addition of co-adsorbents like chenodeoxycholicacid (CDCA) that dissolved in the sensitizing dye solution and prevent aggregation of the dyes was introduced to overcome thi sproblem. The CDCA molecules co-adsorb to the oxide surface with the dye, preventing aggregate formation and increase electron injection, hence improve the photocurrent (Manthou et al., 2015). The enlargement of the optical path length by adding larger diffusive particles to the film and varying the thickness of the semiconductor layer are another way to increase the efficiency (Deepak et al., 2014). However, for the most typical materials for photoanodes in DSSC (nanoparticles of TiO_2) the charge transport is relatively slow, decreasing the efficiency for thick layers. Therefore, by varying morphologies and architectures (nanoparticles, nanotubes, nanowires, core–shell structures), including those with alternative types of semiconductors (e.g. ZnO or SnO_2), have been developed to improve the electron mobility in the photoanode (Concina et al., 2015; Omar et al., 2015; Ye at el., 2015). Moreover, the multifuncionality and ability to improve the charge transport and collection processes of carbon-based materials (especially graphene) make them also appropriate for the use in photoanodes.

2.3.2 Optimizing of open circuit voltage (V_{OC})

In order to increase the efficiency of DSSC, it is important to maximize the light to electric energy conversion efficiency by maximizing the photocurrent while keeping the photovoltage high (Ning et al., 2010). Therefore, modifying types of semiconductor, thickness and morphologies of the film have been used to obtain high V_{OC} without decreased the J_{SC} value (Tetreault et al., 2012; Concina et al., 2015).

Thus, if further improvement in DSSCs efficiency will be realized, the working mechanisms in the complete devices must be explored.

2.4 Sensitizer (Dye)

The sensitizer (dye) has the role in absorbing and converting the solar energy to electrical energy. The dye is chemically bound to the TiO_2 surface (the semiconductor). The selected dye has to meet several requirements to be considered as an efficient sensitizer such as able to absorb a broad range of the incident light, and strongly binding onto the TiO_2 surface. The selection of the dye also need to match with the lowest unoccupied molecular orbital (LUMO) to the edge of the conduction band of TiO_2 and have lower highest occupied molecular orbital (HOMO) compared to the redox potential of electrolyte. Moreover, the molecular structure of the dye also affects the performance of the solar cell (Anandan, 2007; Gong et al., 2012; Narayan, 2012). The sensitizers are mainly categorized into three groups; metal complex sensitizers, metal-free organic sensitizers and natural sensitizers.

2.4.1 Metal Complex Sensitizer

In DSSCs, metal complex sensitizer such as polypyridyl ruthenium are used widely and studied for its outstanding redox properties, high stability and good response to natural visible sunlight. It may be divided into carboxylate polypyridyl ruthenium dye, phosphonate ruthenium dye and poly nuclear bipyridyl ruthenium dye. The first two types of sensitizers lie in the adsorption group and it differs from the last types of sensitizers in the number of metal center. The carboxylate polypyridyl ruthenium dye is in level structure and easily to be desorbed from the surface in the aqueous solution. Therefore, it allows the electron injection into the

conduction band of the semiconductor (Kong et al., 2007). More than 11% efficiency recorded are based on N719 or black dye (Mao et al., 2012).

The use of squaraine dye as co-sensitizer of ruthenium polypyridyl complexes obtained 13% photo current efficiency (PCE) for DSSCs than those with simple ruthenium polypyridyl complexes. By co-sensitization of polypyridyl ruthenium dye and squaraine dye in a proper ratio, a higher PCE was recorded (Wei at el., 1999; Zhao et al., 1999). The N3 dyes as a sensitizer is almost unmatched until the emergence of black dye. The synthesis of black dyes is performed by panchromatic sensitization character over the whole visible range (near IR region up to 920 nm) (Nazeeruddin et al., 1997). At present, the highest efficiency of approximately 11.15% with an area of 0.219 cm under standard AM 1.5 illumination achieved by using black dye N749 (Chiba et al., 2006).

Although, metal complex sensitizers (e.g. ruthenium (II) based sensitizers) provide a relatively high efficiencies and stability, they are several problems associated with them, example; high production cost besides a long synthesis and purification steps. These problems can be overcome by applying metal-free organic dyes in DSSCs instead of metal complex sensitizers (Faccio et al., 2011).

2.4.2 Metal-Free Organic Sensitizer

Recently, the attention has been given on organic dye development due to its energy conversion efficiency is comparable with polypyridyl ruthenium dye where the improvements in the energy conversion efficiency, from 4% to 9% for organic dyes based DSSCs (Chen et al., 2007; Ooyama et al., 2009). The main advantage associated with organic dyes is the ease in structural modifications which can improve the efficiency in DSSC. In addition, organic sensitizers usually show

considerably higher extinction coefficients compared to metal-based complexes such as ruthenium complex sensitizers (Hagfeldt et al., 2010).

The general design of a metal-free organic sensitizer is a donor-acceptor-substituted π-conjugated bridge (D-π-A) (Figure 2.1). The properties of a sensitizer vary on the electron- donating ability of the donor part and the electron-accepting ability of the acceptor part, as well as on the electronic characteristics of the π bridge. At present, most of the π bridge conjugated part in organic sensitizers are based on oligoene, coumarin, oligothiophene, fluorene, and phenoxazine (Hara et al., 2003; Kitamura et al., 2004). The donor part have been synthesized with a dialkyl amine or diphenylamine moiety while using a carboxylic acid, cyanoacrylic acid or rhodanine-3- acetic acid moiety for the acceptor part (Chen et al., 2007; Ooyama et al., 2009). As shown in Figure 2.3, the sensitizer anchors onto the porous network of nanocrystalline TiO_2 particles via the acceptor part of dye molecule.

Yella et al. (2011) synthesized a donor-π bridge-acceptor (D–π–A) zinc porphyrin dye (YD2-o-C8) which suppresses the interfacial electron back transfer from the nanocystalline TiO_2 film to the oxidized cobalt mediator. The efficiency of the DSSC sensitized with YD2-o-C8 was 12.3% under simulated AM1.5 solar illumination. Mathew et al. (2014) using molecularly engineered a porphyrin which featured the prototypical structure of a donor–π-bridge–acceptor, and this resulted in a landmark efficiency of 13% with $[Co(bpy)_3]^{2+/3+}$ redox couple under simulated AM1.5 solar illumination.

However, the organic dyes also have several disadvantages, which raise the question as whether they are suitable for long-term use in DSSCs. The major drawbacks associated with metal free organic sensitizers (Hagfeldt et al., 2010) are:

i. Strong π-stacked aggregates between D–π–A dye molecules on TiO_2 surfaces, which reduces the electron-injection yield from the dyes to the CB of TiO_2

ii. Low absorption bands compared to metal-based sensitizers, which leads to a reduction in the light absorption capability,

iii. Considerably low stability due to the sensitizers' tendency to decay with time.

iv. Long tedious purification process.

v. Dyes themselves could be toxic or their by-products may act as environmental pollutants.

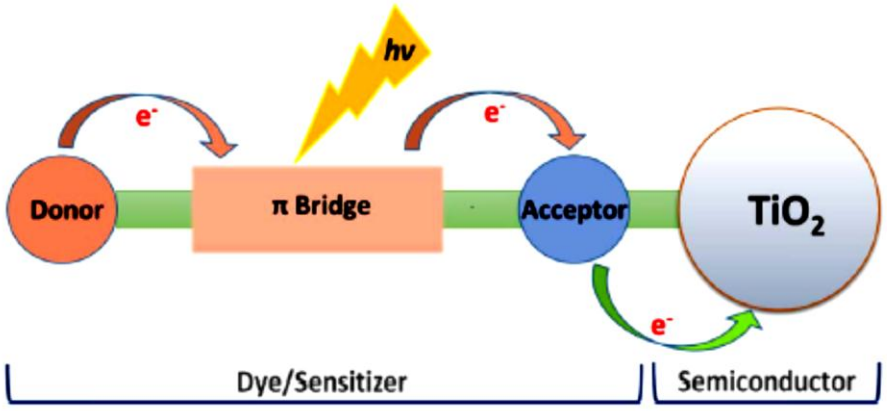

Figure 2.3: Designed structure of a metal-free organic dye (Kumara et al., 2017)

2.4.3 Natural Dyes Sensitizers

Natural dyes can be easily extracted from fruits, flowers and leave exhibit various colour and can be employed in DSSC. Using natural dyes as photosensitizers can reduce the cost as it does not involve noble metals such as Ru (Kimura et al., 2012). Another advantages also, the natural dyes have large absorption coefficients in visible region, easy to prepare and environmental friendliness (Hemalatha et al., 2012). Pigments that extract from the plants exhibit electronic structure that able to

interact with sunlight (due to photosynthesis process) and alters the wavelengths that either transmitted or reflected by the plant tissue. This process leads to the occurrence of plant pigmentation and each pigments is described from the wavelength of the maximum absorbance (λ_{max}) and the color perceived by humans (Hamadanian et al., 2014). The absorption in the visible or near-infrared regions of the solar spectrum and the binding to the semiconductor TiO_2 are important for photosensitizers to function in DSSC (Maurya et al., 2016). The functional group necessary to interact with the TiO_2 surface is a carboxylic or other peripheral acidic anchoring group (Wang et al., 2005; Kumara et al., 2013). The best anchoring groups for metal oxides are carboxylic acid and their derivatives such as acid chlorides, amides and esters (Narayan et al., 2011). Figure 2.4 shows the flow chart diagram about classification of pigments present in plants.

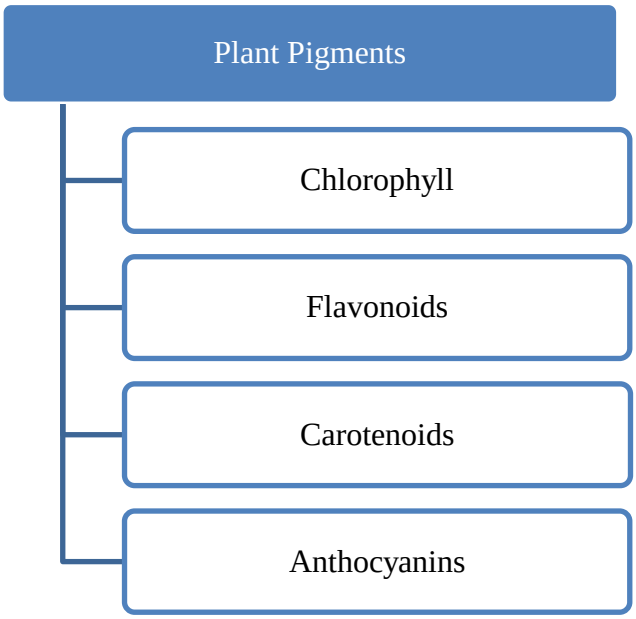

Figure 2.4: Classification of plant pigments

In addition to the light absorption and the high temperature stability, the dye should fulfill the requirement of the efficient electron injection (Suhaimi et al., 2015). Therefore, the functional group of the dyes has been modified at the molecular level. An anchoring group plays an important role to enhance the photovoltaic properties. Efficient carrier injection requires proximal contact between the dye and photoanode. Carboxylic acid and phosphonic acid are typical anchoring groups, a difference in the proximity makes the electron move two times faster in carboxylic acid anchor compare to phosphonic acid. The polarity of the dye semiconductor interface needs to be controlled to increase the carrier injection. Minimize aggregation within the photoanode is another factor that need to be considered. It is because aggregation reduces the carrier injection efficiency. Hence, it is important to prevent aggregation. For instance, dye molecules with a smaller number of a carboxyl group have less chance to form intermolecular aggregate which comes from hydrogen bonding between carboxyl group of the dye molecules.

Although these natural dyes are suitable for the DSSCs, a major constraint associated with their chemical structure limits the research to some extent. This is because the natural pigments are developed through natural evolution and their structural arrangement is difficult to change in vitro (Al-Ghamdi et al., 2014). To overcome this limitation, certain alternatives are identified to maximize the function of those dyes in DSSC. Modification of extraction techniques, application of different sensitization methods (e.g.: co-sensitization) and concentration or pH changes can enhance the function of natural dyes in DSSC. Another alternatives such as optimizing the size of TiO_2 nanoparticles or the thickness of TiO_2 film, optimizing soaking time of TiO_2 electrode in pigments solution and adjusting the electrolyte composition also can increased the photovoltaic performance using natural dyes

(Warkoyo et al., 2011; Kumara et al., 2013, 2015; Lim et al., 2015; Lim et al., 2015; Shalini et al., 2015; Hosseinnezhad, 2016).

2.4.3.1 Chlorophyll

Chlorophyll is a green pigment that found mostly in green plants. Harvesting of light energy and converting solar energy to chemical energy are primary functions of chlorophyll. Chlorophyll includes a group more than 50 tetrapyrrolic pigments (Wang et al., 2005). The most efficient types of chlorophyll are chlorophyll α (chlorine 2) due to their derivative are inserted into DSSC as sensitizers because of their beneficial light absorption tendency modes (Scheer, 2003). Zhou et al. (2011) reported that chlorine 2 has ability to lead semiconductor TiO_2 and ZnO surfaces through different modes.

2.4.3.2 Flavonoids

Flavonoids are the most widespread and physiologically active group of natural constituents that are important in contributing color to flowers (Middleton et al., 1993). Flavonoids has a basic C_6-C_3-C_6 skeleton as shown in Figure 2.5. There is a limitation to the number of flavonoid structures that found in nature which vary in their states of oxidation from flavan-3-ol to flavonols and anthocyanins. Flavonoids also include flavanones, flavanonols and flavan-3, 4-diols (Swain, 1976).

The charge transfer transitions from HOMO to LUMO for flavonoids require less energy, energizing the pigment molecules by visible light, leading to a broad absorption band in visible region (Maher et al., 2006). The various flavonoid pigment colour are determined by the wavelength of visible light that absorbed by pigment molecules and reflected. The flavonoid gets rapidly adsorbed to the mesoporous TiO_2 surface by displacing an OH- counter ion from the Ti site that